Proc. of the 9th Intl. Conf. of Asian Society for Precision Engg. and Nanotechnology (ASPEN 2022)
15–18 November 2022, Singapore. Edited by Nai Mui Ling Sharon and A. Senthil Kumar
doi://10.3850/978-981-18-6021-8_OR-12-0011

Visualization of Graphene Mineral Oil Immersion Cooling for Electric Vehicle Battery Temperature Analysis

Ya-Chi Ho[1,#], Po-Chih Chen[1], Yung-Jen Cheng[1], Cheng-Ting Hsu[1], and Da-Jeng Yao[1]

1 Mechanical and Mechatronics Systems Research Labs., Industrial Technology Research Institute, 195, Sec. 4, Chung Hsing Rd., Chutung, Hsinchu, Taiwan 310401, R.O.C.
Corresponding Author / Email: Light.Ho@itri.org.tw, TEL: +886-3-591-6620, FAX: +886-3-582-0456

KEYWORDS: Immersion cooling, Graphene, Battery temperature, Electric vehicle, Visualization

As the heat generation power of the batteries increases with the improved performance of electric vehicles, effective thermal management is required. The overall temperature uniformity of the battery pack is important, and immersion cooling has become an important thermal solution, immersing the battery directly in the dielectric liquid. With the introduction of graphene, the thermal conductivity of the dielectric liquid increases significantly. In this study, the graphene at 100 nm and mass concentration of 0 to 0.5wt% in mineral oil is used. According to the numerical simulation analysis, the effect of battery temperature is simulated when the battery is charged and discharged at 1C, 2C, 3C and 4C. Furthermore, the visual test platform is used to shoot the experimental state and test temperature data, and test the liquid resistance to study the feasibility of graphene in immersion cooling.

NOMENCLATURE

q = battery heating rate (W)
I = current (A)
V_b = effective calculated volume of the battery cell (m^3)
U = the test voltage of the battery cell (V)
U_0 = open circuit voltage of battery cell (V)
T = temperature (℃)
C = the charge and discharge current of the battery
T1–T4 = thermocouples (-)

1. Introduction (Times New Roman 10pt)

Net-zero carbon emissions have become a global consensus on environmental development. Facing this wave, all countries are committed to developing electric vehicles [1] to achieve the goal of net-zero carbon emissions. As a key component of the energy storage and power source of electric vehicles, batteries have become the focus of research and development by major manufacturers. As the power density of the battery increases year by year, the heat generation value of the battery increases year by year. If the temperature of the battery exceeds 45℃, it will damage the performance of charging and discharging [2]. Excessive temperature will cause the battery to catch fire, which will seriously endanger the safety of personnel. Therefore, how to quickly and massively conduct heat away from the battery to effectively dissipate heat has become an important research topic.

The introduction of nanofluids into the field of heat dissipation originated from the publication of the General Theory of Electromagnetics by Maxwell [3]. In addition to integrating the theory of electromagnetic properties, it also brought a new concept of mixed-liquid two-phase flow of particles in the fluid. Although it was impossible to produce nanofluids in the early 20th century, Maxwell used theoretical predictions to add circular particles to the suspension liquid, and the thermal conductivity was improved. In the middle of the 20th century, Hamilton and Crosser [4] believed that heat transfer should occur on the particle surface, so they controlled the particle shape and surface area, revised the Maxwell model, and further increased the thermal conductivity. In 1975, Ahuja [5] studied the effect of particle volume, size and flow rate on heat conduction. However, at that time, it was not possible to produce nanoparticles, and even no suitable suspending agent could be used for proper separation of nanoparticles in fluids. Micron- and millimeter-sized particles were merely added to the working fluid, and the thermal conductivity was found to increase, verifying that Maxwell's theoretical prediction was correct. Unfortunately, due to the large particle size, micron and millimeter-sized particles eventually appeared in the experiment, which blocked the pipeline and even

caused the pipeline to wear.

At the end of the 20th century, nanotechnology gradually matured, and Choi [6] became the first to use copper oxide nanofluids and titanium dioxide nanofluids to explore thermal conductivity in nanofluids, improving the previous lack of micro- and millimeter-particles. At present, among nanomaterials, graphene has the best thermal conduction efficiency, which can reach 5,300W/mK, which is much higher than that of nanometer copper oxide powder and nanometer alumina powder.

You et al. [7] studied the effect of nanopowder on the critical heat flux when the nanofluids was boiling in the pool, and found that the critical heat flux of the nanofluids was about twice that of water. Kwark et al. [8] studied nanofluids with low concentrations (≦1g/L), and found that nanoparticles were deposited on the heated surface with a very thin nanoparticle layer, which produced the heat transfer of nucleate boiling in the thin nanoscale region. Wong et al. [9] designed a visualized flat heat pipe, the upper end is a glass flat plate, and the bottom is a mesh capillary structure. The vacuum pumping and perfusion of nano-alumina fluid and nano-copper powder fluid are performed. It was found that the maximum heat transfer rate of nanofluids was 20% higher than that of pure water, resulting in a little boiling. Wong et al. [10] used a visualized flat heat pipe and used a high-speed camera to take pictures of the evaporation area, and observed the heating condition of the evaporation area in the case of acetone and methanol in nano-alumina fluid and nano-copper powder fluid. The experimental results show that with the increase of nano-alumina or nano-copper powder in the working fluid, the boiling bubble velocity in the evaporation area increases, thereby improving the thermal conductivity and reducing the evaporation thermal resistance.

J. Mitrovic [11] used a heating cylinder, immersed in the liquid, to give different watts of heat. When the cylinder surface is smooth, as the heat flux increases, the temperature difference between the temperature inside the cylinder and that on the cylinder surface becomes larger and larger, which means that the heat transfer effect is not good; on the contrary, the cylinder surface is given roughness. As the heat flux increases, the temperature difference between the temperature inside the cylinder and that on the surface of the cylinder is almost constant, which means that the heat transfer effect is better. Moreover, in the experimental tests on four parts of the cylinder, the results indicate that the heat transfer with the rough surface is better than that of the smooth surface. The main reason is that there will be many nucleation sites on the rough surface. When the cylinder is heated, the nucleation sites will generate nucleate boiling, which will increase the heat exchange and reduce the temperature difference between the inside and outside of the cylinder.

Immersion cooling can be applied to solar panels, data centers, electric vehicle battery cooling and other issues [12], and can improve space temperature uniformity, save cooling energy, and save cooling costs. Charlotte Roe [13] et al. conducted a literature review on immersion cooling for lithium batteries. Qingyi Luo [14] used silicon carbide oil based nanofluids for the data center immersion cooling to study its optimal heat dissipation. Suhaib Umer Ilyas [15] et al. analyzed the rheological behavior of diamond-graphene doped in mineral oil, and found that viscosity was significantly affected by concentration, temperature, shear rate and surfactant. R. Dinesh [16] studied and simulated the thermal rheological behavior of graphene oxide on mineral oil nano-humidifiers and found that at 0.75vol%, the thermal conductivity and dynamic viscosity were increased to 70% and 50%, respectively.

2. Experimental Methods (Times New Roman 10pt)

2.1 Battery heat

Yuqi Huang, et al. [17] studied the heat generation during battery discharge. The heating rate of a single cell during discharge can be calculated by Bernadi's equation, as shown in equation (1). Battery heating rate per unit time and unit volume q (W/m^3) is

$$q = \frac{1}{V_b}\left[I^2 R_0 + IT\frac{dU_0}{dT}\right] \quad (1)$$

where I is the current through the battery, positive when charging and negative when discharging. V_b is the effective calculated volume of a single battery cell. U and U_0 are the test voltage and open circuit voltage of the battery cell, respectively. T is the current battery temperature. T_dU_0/dT is a parameter related to the electrochemical reaction, called the temperature coefficient. The internal resistance can be set to 0.04Ω, and T_dU_0/dT can be set to 0.01116V. The heating rate under different discharge conditions can then be calculated as a constant value. For example, to calculate the heat generation rate of a single 18650 battery under discharge, the 1C discharge current is 1.35A. The diameter of a single 18650 battery is 1.8cm and the height is 6.5cm, so the volume V_b is 1.654×10^{-5}m^3. Assuming that the inner group is 0.04Ω and T_dU_0/dT is 0.01116V, the heating rate q per unit volume of a single battery is 0.087966W. If the heat generation rate of a single 18650 battery under discharge is calculated, and the 2C discharge current is 2.70A, the heat generation rate q per unit volume of a single battery is 0.321732W. By analogy, the heating rate q per unit volume of a 3C single battery is 0.701346W; the heating rate q per unit volume of a 4C single battery is 1.226744W.

2.2 Experimental Architecture

In the experimental design, the battery model was made of red copper, with a diameter of 1.8cm and a height of 6.5cm, and a heating rod placed in the center with a diameter of 0.65cm and a height of 5.0cm. Additionally, laying out the thermocouples, these thermocouples, K-type 1mm-diameter (Omega, Inc.), are denoted by T1-T4, respectively. T1 fits tightly on the heating rod and uses TIM to lower the air thermal resistance of the heating rod, thermocouples and the inner wall of the battery model, and the thermal conductivity of TIM is 1W/m-K. T2 is on the surface of the heating rod, T3 is the temperature change of the immersion liquid, and T4 is the ambient temperature, as shown in Figure 1. The overall experimental architecture, in the chamber of immersion cooling, adopts a transparent design on all sides as a visual study. Below the transparent chamber is a chamber with a built-in pump, which can transport the cold fluid below to the right side of the transparent chamber above. A

flow channel is designed on the left side of the transparent chamber to allow the heated fluid to use gravity from above to reflux to the bottom for cooling, as shown in Figure 2 for the experimental structure and Figure 3 for the actual product.

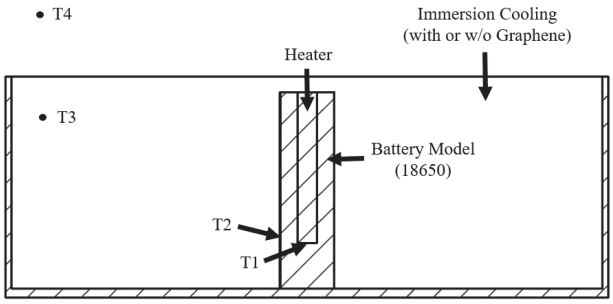

Fig. 1 The battery and immersion cooling along with thermocouple positions

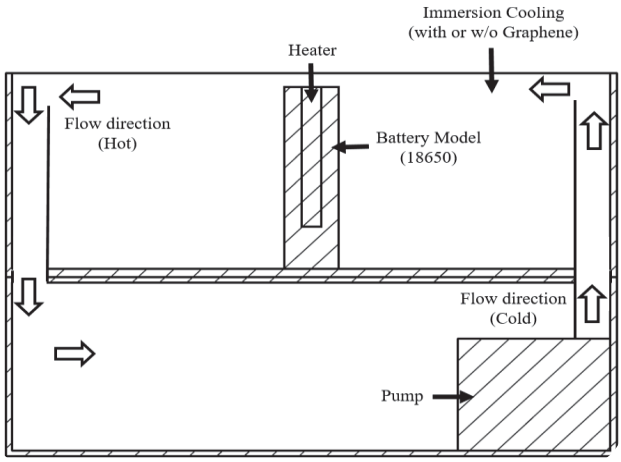

Fig. 2 Overall experimental setup

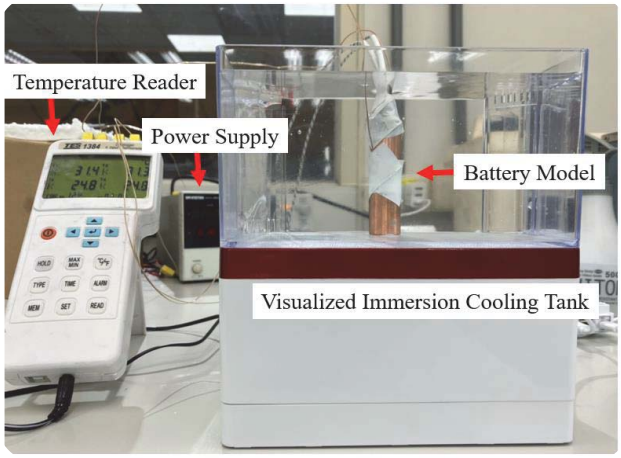

Fig. 3 Overall experimental entity setup

2.3 Graphene Immersion Cooling Process and Insulation Testing

Using chemical vapor deposition, methane and nitrogen are passed through Remote Plasma Source (RPS) to make graphene under plasma. Subsequently, the vacuum pump and filter are used to separate the gas and graphene powder. The process is shown in Figure 4. The graphene powder was removed and mixed with mineral oil without active agent. Each set of experiments was completed within two hours after mixing. The proportion of added graphene powder is within 2.5 wt%. After the graphene and the working fluid were mixed, they were stirred with an electromagnetic stirrer for 60 minutes, followed by ultrasonic vibration for 8 hours, and the temperature was maintained at 25°C. This process facilitates the uniform dispersion of graphene in mineral oil.

Mineral oil is an insulator, and although graphene is a good conductor, a small amount and evenly dispersed in the fluid will not cause a path. Different weights of graphene powder are added to 100ml of mineral oil to test the conductivity of the fluid, as shown in Figure 5. The resistance value can be measured inside the fluid above 0.5wt%, and the reciprocal of the resistance value is 0 below 0.5wt%. Therefore, to test the concentration of graphene immersion cooling, choose between 0-0.5wt%.

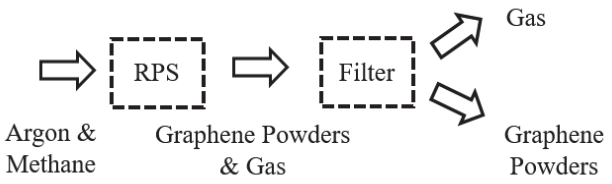

Fig. 4 Graphene production

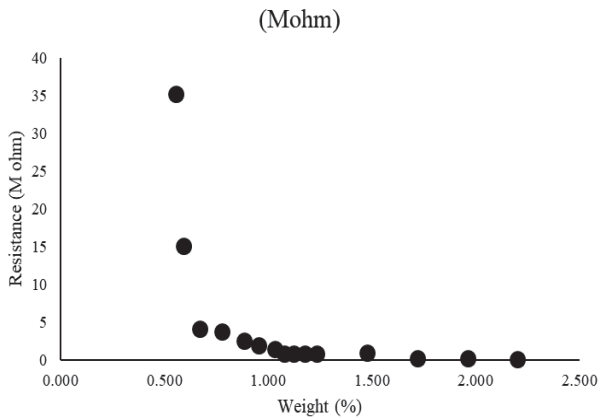

Fig. 5 Graphene mineral oil – weight% and resistance

The visual shooting part uses a 12-megapixel wide-angle lens with an F1.8 aperture. The purpose of the shooting is to observe whether the graphene nanopowders has an effect on the mineral oil when heated.

3. Experimental Results

During the actual measurement, the battery is given the unit volume heating rate of 0.087966W, 0.321732W, 0.701346W, 1.226744W. The corresponding battery charge and discharge are 1C, 2C, 3C and 4C. Using mineral oil and adding 0.025wt% and 0.1wt%

graphene concentration to compare the temperature of the battery model immersion cooling, the test is 20 minutes, and the battery model temperature reaches a steady state after about 15 minutes. It can be seen from Figure 6 that at different heating wattages, the temperature of the battery in 0.025wt% graphene-mineral oil is lower than that in mineral oil; while the battery in 0.1wt% graphene-mineral oil is lower than pure mineral oil. The temperature inside is higher. Figure 6(a), the temperature of the battery in 0.025wt% graphene-mineral oil is 0.2°C lower than that in mineral oil, and the temperature of the battery in 0.1wt% graphene-mineral oil is 0.4°C higher than that in mineral oil; Figure 6(b), the temperature of the battery in 0.025wt% graphene-mineral oil is 0.2°C lower than that in mineral oil, and the temperature of the battery in 0.1wt% graphene-mineral oil is 0.2°C higher than that in mineral oil; Figure 6(c), the temperature of the battery in 0.025wt% graphene-mineral oil is 0.6°C lower than that in mineral oil, and the temperature of the battery in 0.1wt% graphene-mineral oil is 0.2°C higher than that in mineral oil; Figure 6(d), the temperature of the battery in 0.025wt% graphene-mineral oil is 0.6°C lower than that in mineral oil, and the temperature of the battery in 0.1wt% graphene-mineral oil is 0.2°C higher than that in mineral oil.

Adding a small amount of graphene to mineral oil has a significant cooling effect. However, when the graphene concentration is increased in mineral oil, the heat dissipation effect is poor. It is speculated that the viscosity of the fluid increases, which makes the fluid flow difficult, resulting in poor heat dissipation.

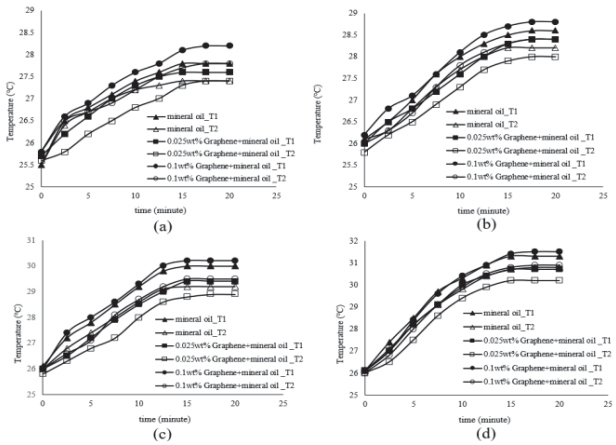

Fig. 6 Experimental Result : (a) Battery discharge 1C ;(b) Battery discharge 2C ;(c) Battery discharge 3C ;(d) Battery discharge 4C

Using the same pump, perform actual measurements at different temperatures, and observe the flow rate of the working fluid per minute. The fluid is water, mineral oil, mineral oil mixed with 0.025wt% graphene, and mineral oil mixed with 0.1wt% graphene, as shown in Figure 7. Compared with pure mineral oil, the mineral oil mixed with 0.025wt% graphene reduces the flow rate per minute by about 10%, while the mineral oil mixed with 0.1wt% graphene has a flow rate per minute compared with pure mineral oil. A reduction of about 26%. Due to the high concentration of graphene, the viscosity increases, the flow velocity decreases, and the heat exchange efficiency decreases.

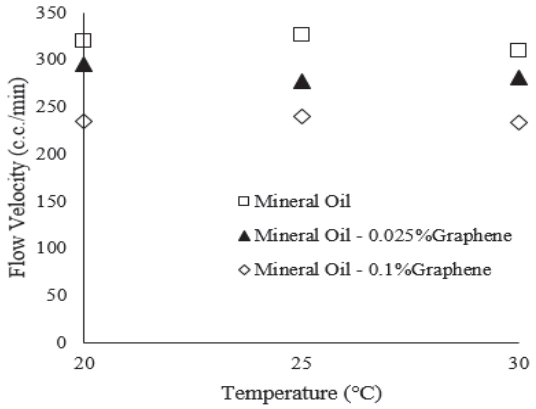

Fig.7 Fluid viscosity causes flow velocity at different temperatures

It can be found from Figure 8 that when 0.025wt% graphene and mineral oil are used for immersion cooling of the battery model, part of the graphene powder adheres to the battery model, part of it moves during the flow, but part of it gathers on the battery model, so that the random mode occasionally leaves the battery model. Graphene powder helps heat conduction on the battery model and increases the heat specific capacity, but it increases the fluid viscosity, which reduces the heat exchange rate.

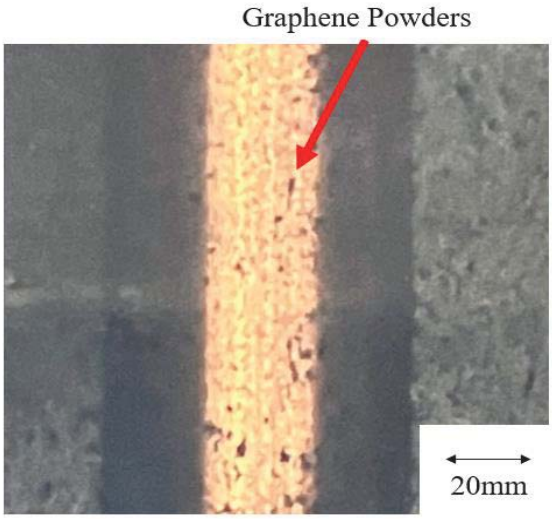

Fig.8 Visualizing graphene immersion cooling

4. Conclusions (Times New Roman 10pt)

According to the above experiments, the nanofluids conductivity analysis corresponding to different graphene concentrations, the working fluid flow analysis corresponding to different graphene concentrations, and the temperature conditions of the battery model under the heat generation value of different battery models were carried out. A few conclusions are drawn:

1. Graphene is mixed with mineral oil, and the conductivity needs to be considered. In order to allow the nanofluids to carry out immersion cooling of the battery, it cannot have

electrical conductivity, so the graphene concentration can only be below 0.5wt%.

2. Graphene powder is produced by chemical vapor deposition method, and the thickness can reach 100nm. Therefore, increasing the amount of graphene added leads to an increase in the viscosity of the nanofluids. Adding 0.025wt% graphene causes the flow per minute of the working fluid under the same pump to decrease by 10%; adding 0.1wt% graphene, the flow per minute decreases by 26%.
3. In 0.025wt% graphene nanofluids immersion cooling at the heat generation value of 1C, 2C, 3C and 4C, the temperature is 0.2~0.6℃ lower than mineral oil immersion cooling; in 0.1wt% graphene nanofluids immersion cooling at the heat generation value of 1C, 2C, 3C and 4C, the temperature is 0.2~0.4℃higher than that of mineral oil immersion cooling.
4. The 0.025wt% graphene nanofluids immersion cooling is better than 0.1wt% graphene nanofluids immersion cooling. It is speculated that graphene increases thermal conductivity and thermal specific capacity, but too high concentration makes the flow rate slow down and heat exchange decline instead.

ACKNOWLEDGEMENT

This work was financially supported by Industrial Technology Research Institute (ITRI), ROC under Contract M101WT7000.

REFERENCES

1. E. Doroudchi, K. Alanne, Ö. Okur, J. Kyyrä and M. Lehtonen, “Approaching net zero energy housing through integrated EV,” Sustain. Cities Soc., vol. 38, pp. 534–542, Apr. 2018.
2. C. Chu, B.W. Kwon, W. Lee and Y. Kwon, “Effect of temperature on the performance of aqueous redox flow battery using carboxylic acid functionalized alloxazine and ferrocyanide redox couple,” Korean J. Chem. Eng., vol. 36, no. 10, pp. 1732–1739, Oct. 2019.
3. C. Maxwell, *A Treatise on Electricity and Magnetism*, 2nd Ed., Oxford University Press, New York, pp. 435–441, 1904.
4. R. L. Hamilton and O. K. Crosser, “Thermal conductivity of heterogeneous two-component systems,” Ind & Engr. Chem. Fundamentals, vol. 1, pp. 187–191, 1962.
5. A. S. Ahuja, “Augmentation of heat transfer in laminar flow of polystyrene suspension,” J. Appl. Phys., vol. 46, pp. 3408–3425, 1975.
6. S. U. S. Choi, “Enhancing thermal conductivity of fluids with nano-particles,” in ASME IMECE, pp. 99–105, 1995.
7. S. M. You, J. H. Kim and K. H. Kim, “Effect of nano-particles on critical heat flux of water in pool boiling heat transfer,” Appl. Phys. Lett., vol. 83, pp. 3374–3376, 2003.
8. A. M. Kwark, R. Kumar, C. Moreno, J. Yoo and S. M. You, “Pool boiling characteristics of low concentration nanofluids,” Int. J. Heat Mass Transfer, vol. 53, pp. 972–981, 2010.
9. S.-C. Wong and Y.-C. Ho, “Visualization experiment on the evaporation characteristics in nanoparticle-laden mesh-wicked heat pipe,” Frontier in Heat Pipes (FHP), vol. 4, 023001, 2013.
10. S.-C. Wong and Y.-C. Ho, “Visualization for heat pipe evaporator of nanoparticle laden mesh wick with water, methanol or acetone,” in Proceedings of the 1st Thermal and Fluid Engineering Summer Conference (TFESC-12806), pp. 2023–2029, 2015.
11. J. Mitrovic, “How to create an efficient surface for nucleate boiling,” Int. J. Ther,. Sci. vol. 45, pp. 1–15, 2006.
12. N. A. Pambudi, A. Sarifudin, R. A. Firdaus, D. K. Ulfa, I. M. Gandidi and R. Romadhon, “The immersion cooling technology Current and future development in energy saving,” Alex. Eng. J., vol. 61, pp. 9509–9527, 2022.
13. G. Roe, X. Feng, G. White, R. Li, H. Wang, X. Rui, C. Li, F. Zhang, V. Null, M. Parkes, Y. Patel, Y. Wang, H. Wang, M. Ouyang, G. Offer and B. Wu, “Immersion cooling for lithium-ion batteries – A review,” J. Power Sources., vol. 525, 231094, 2022.
14. Q. Luo, C. Wang, H. Wen and L. Liu, “Research and optimization of thermophysical properties of sic oil-based nanofluids for data center immersion cooling,” Int. Commun. Heat Mass Transf., vol. 131, 105863, 2022.
15. S. U. Ilyas, S. Ridha, S. Sardar, P. Estelle, A. Kumer and R. Pendyala, “Rheological behavior of stabilized diamond-graphene nanoplatelets hybrid nanosuspensions in mineral oil,” J. Mol. Liq., vol. 328, 115509, 2021.
16. R. Dinesh, P. Karuppasamy and S. Kalaiselvam, “An experimental investigation and comprehensive modelling of thermal and rheological behaviour of graphene oxide nano platelets suspended mineral oil nano lubricant,” J. Mol. Liq., vol. 347, 118357, 2022.
17. Y. Huang, Y. Lu, R. Huang, J. Chen, F. Chen, Z. Liu, X. Yu and A. P. Roskilly, “Study on the thermal interaction and heat dissipation of cylindrical lithium-ion battery cells,” Energy Procedia, vol. 142, pp. 4029–4036, 2017.